Journal of Magnetics 8(1), 50-59 (2003)

An Optical Micro-Magnetic Device: Magnetic-Spatial Light Modulator

Jae-Hyuk Park*[1,4], M. Inoue[1,3], Jae-Kyeong Cho[2], K. Nishimura[2] and H. Uchida[2]

[1]*Electrical & Electronic Engineering, Toyohashi University of Technology, 1-1 Hibari-Ga-Oka, Tempaku, Toyohashi 441-8580, Japan*
[2]*Electronic Materials Engineering, Gyeongsang National University, 900 Gajwa-dong, Jinju, Gyeongnam 660-701, Korea*
[3]*JST-CREAST,* [4]*ASTF*

(Received 10 December 2002)

Spatial light modulators (SLMs) are centrally important devices in volumetric recording, data processing, pattern recognition and other optical systems. Various types of reusable SLMs with two-dimensional pixel arrays have been intensively developed. Of these, magneto-optic spatial light modulators (MOSLMs) have advantages of high switching speed, robustness, nonvolatility, and radioactive resistance. In this article, we review recent development work on MOSLMs, mainly in relation to our own studies.

Key words : spatial light modulator, magneto-optical effect, metal stress, micro-magnetic device, volumetric optical recording

1. Introduction

A spatial light modulator (SLM) is real-time programmable device capable of modifying the amplitude, phase or polarization of an optical wave front as a function of position *via* electrical or optical control signals. Various types of reusable SLMs with two-dimensional pixel arrays, which are ferroelectric liquid crystal SLM (FLC-SLM), deformable mirror device (DMD), grating light valve (GLV), TMA, magneto-optic SLM (MOSLM) and multiple quantum well SLM, are centrally important devices in holography optical data storage, data processing, pattern recognition, optical computer and other optical systems. Of these, the magneto-optic spatial light modulators are magneto-optical device modifying the plane of polarization of light rays by the Faraday rotation effect from a LPE epitaxial garnet film.

The MOSLMs have advantages of high switching speed, robustness, nonvolatility, and radioactive resistance. The high switching speed in MOSLMs results from the fact that the pixel switching of magnetization direction, up or down, can be performed within the order of 1 ns. The MOSLM, which is a robust solid state device, is also nonvolatility because the pixels are not spontaneously demagnetized even after shutting off the electric power [1, 2].

The first commercialized MOSLM was the Litton iron garnet H (magnetically) triggered magneto-optical device (LIGHT-MOD) developed by Ross *et al.* at Litton two decades ago [3, 4]. It consisted of an array of square garnet pixels; that were electrically addressed using X-Y matrix drive conductors. It thus had high switching speed and high stability of the written information. However, it needed a rather high drive current to produce a magnetic field sufficiently high for nucleating a domain wall. It operated in the transmission mode and featured large gaps between the pixels in order to provide space for the X and Y drive conductors which occupied the gaps.

The advanced version of the LIGHT-MOD, the reflected mode MOSLM (R-MOSLM), was developed by Cho *et al.* at Litton a decade ago [5]. It also consisted of an array of square garnet pixels that were electrically addressed using X and Y matrix drive conductors but operated in the reflected mode by introducing the X and Y matrix metal layers on top of the pixellated garnet surfaces, which served as both drive conductors and reflective mirrors. The R-MOSLM took advantage of the nonreciprocity of the Faraday effect. Compared to the transmission-mode devices, the film thickness in the R-MOSLM can be halved without losing the image contrast by exploiting the nonreciprocal characteristic of the MO effect.

However, the MOSLM has significant disadvantages as

*Corresponding author: Tel and Fax: +81-532-44-6749, e-mail: park@maglab.eee.tut.ac.jp

© 2003 **Journal of Magnetics**

follows. A large drive current is required to produce a magnetic field enough to nucleate the reversed magnetization at selected pixels. Since a physically isolated pixel has a deep gap produced by ion milling process, a planarization process of the deep gap is required to deposit the conductor lines. Also, the isolated positions in each pixel have to be ion-implanted to reduce external bias field for saturating pixels. Finally, the use of the enveloping bias coil is disadvantageous for several reasons. The bias coil requires the use of an additional component and relatively large amounts of power, and increases the area occupied by the device.

Based upon the above described disadvantages, we have developed new tools to materialize the MOSLM in practical applications including new type drive line for low driving current [6, 7], unique pair-domain by patterned assist permalloy film [8], groove depth controlling method [9], voltage addressing method [10], and flat-surface pixel [11]. In this article, we review recent development work on MOSLMs, mainly in relation to our own studies.

2. Principles of R-MOSLM

The magneto-optic switching element (Mesa) in the MOSLMs is a rectangular array of pixels. The pixels were made of a bismuth-substituted iron garnet film grown on a nonmagnetic single crystal substrate. It is a uniaxial crystal with its uniaxial axis oriented perpendicular to the surface plane of the film. The pixels of a MOSLM must be separated to prevent them from magnetically interacting. This pixel separation is achieved by physically removing the film from the pixels. The separated pixel is also in practice a bistable magnetic domain with an internal magnetic field constantly parallel to the uniaxial axis. The pixel of the MOSLMs is nucleated and demagnetized by the X and Y drive lines and saturated by an external bias coil. In the case of the conventional R-MOSLM, the switching speed of a single pixel was about 10 ns. The magnetic field generated by current flowing in a single drive line is about 200 Oe, which is insufficient to switch the state of a single pixel. A magnetic field of about 400 Oe in combination with the use of X and Y conductors will switch the state of the selected pixel only.. The two stable directions of its internal magnetization can be rapidly switched electrically. The magnetic field generated by current flowing in a single drive line is designed to be insufficient to switch the state of a single pixel. The X and Y drive lines make it possible to switch individual pixels by random selection. That is, the magnetic field combined with X-Y conductors will switch the state of the selected pixel only.

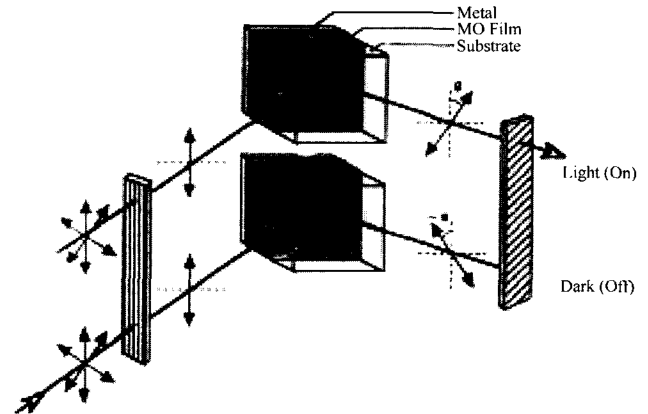

Fig. 1. Reflected mode magnetooptic spatial light modulator device operation.

Figure 1 shows the magneto-optic principle in R-MOSLM devices. When operated, each individual pixel is magnetized in one of the bistable magnetic domain directions. A light ray polarized by a polarizer at the input face enters the nonmagnetic substrate, traverses the MO film, is reflected by the conductors and eventually exits the substrate again. The polarization of the light ray rotates in the same direction as it enters the MO film, say clockwise θ_F, as it does when it is reflected by the conductors and returns through the same film, again clockwise θ_F, resulting in two cycles of the rotation. Its polarization is rotated either twice clockwise, by angle $2\theta_F d$, or twice counterclockwise, by $-2\theta_F d$, depending upon the orientation of the magnetization direction of the separated pixel. Here θ_F refers to the Faraday rotation per unit length and d is the thickness of the MO film. The analyzer set with an angle of $90°-2\theta_F d$ then passes the ray rotated clockwise but blocks the ray rotated counterclockwise. As a result, the pixels appear dark or light. The minimum spacing between the pixel mesas and resolution is directly related to the MO film thickness. Obviously, from a device fabrication standpoint, the thinner the film the higher the resolution that can be achieved. The film thickness in the R-MOSLM can be halved without losing the image contrast by exploiting the nonreciprocal characteristic of the MO effect, compared to the conventional transmission mode.

3. New Tools to Materialize the MOSLM

3.1. Wedge-shaped MOSLM

Figure 2 shows a schematic of the structure of a single pixel of the conventional R-MOSLM and its cross section. The X and Y conductors of the conventional R-

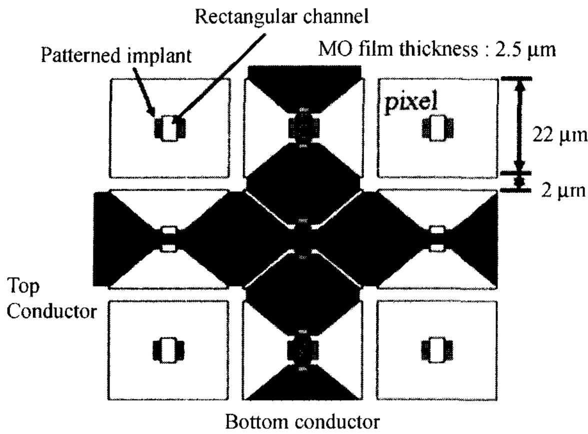

Fig. 2. Schematic of the structure of a single pixel of the conventional R-MOSLM and its cross section.

MOSLM provide a localized, concentrated magnetic field at the point where the conductors cross for reversing the magnetization of the pixel. First, boron ion was implanted at the center of the mesa to reduce the reversal switching field of the pixel and then annealed. At the center of the mesa, a rectangular channel 9.6 μm long, 1.6 μm wide and 0.3 μm deep was ion-milled. The Y conductor was buried the rectangular channel and separated by the patterned SiO_2 insulator pad (6 μm long, 6 μm wide and 0.4 μm thickness) crossing under the X conductor. At this central location, the physical widths of both the X and Y conductors are approximately 1.6 μm and the thicknesses of the X and Y conductors are about 0.4 μm and 0.2 μm, respectively. The X and Y conductors also lie flat on the surface of the mesa forming a mirror.

The drive lines of the conventional R-MOSLM and new R-MOSLM were specially simulated by a 3D electromagnetic field computer simulator. The material of these drive lines is Al. Figures 3 and 4 show the perpendicular magnetic field H_z produced by a driving current of 100 mA at the rectangular cross section (0.2 μm thickness and 2 μm width) of the drive line of the conventional R-MOSLM and the new R-MOSLM, respectively. The three line plots are taken starting at the center of the conductor ($z = 0.1$ μm (a)), at the bottom surface of the conductor ($z = 0.0$ μm (b)) and at 0.2 μm below the conductor ($z = -0.2$ μm (c)). Two observations from Figs. 3 and 4 should be discussed. First, the peak at the center of the conductor ($z = 0.1$ m (a)) is higher by almost a factor of two than the peak below the drive line ($z = -0.2$ μm(c)). Second, the useful perpendicular magnetic field H_z decreases very rapidly as a function of distance from the edge of the drive line. It is only at $x = 0.5$ μm that the magnitude is decreased by almost a factor of two.

For the conventional R-MOSLM, the conductor was

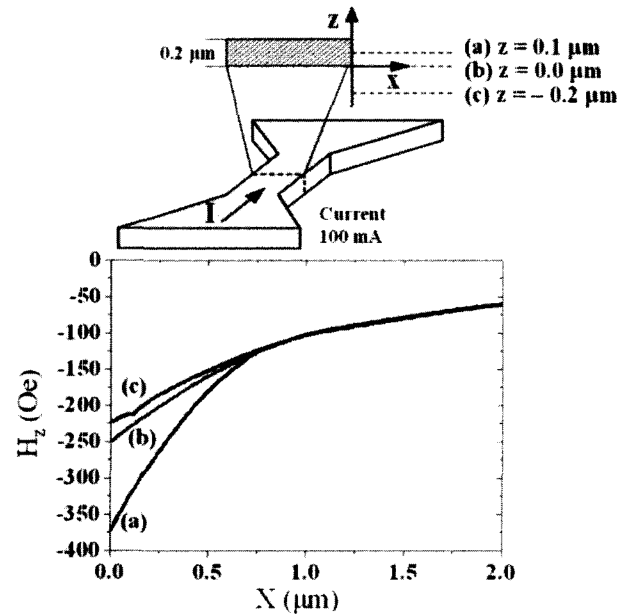

Fig. 3. Perpendicular magnetic field H_z produced by Y drive line of the conventional R-MOSLM carrying 100 mA current.

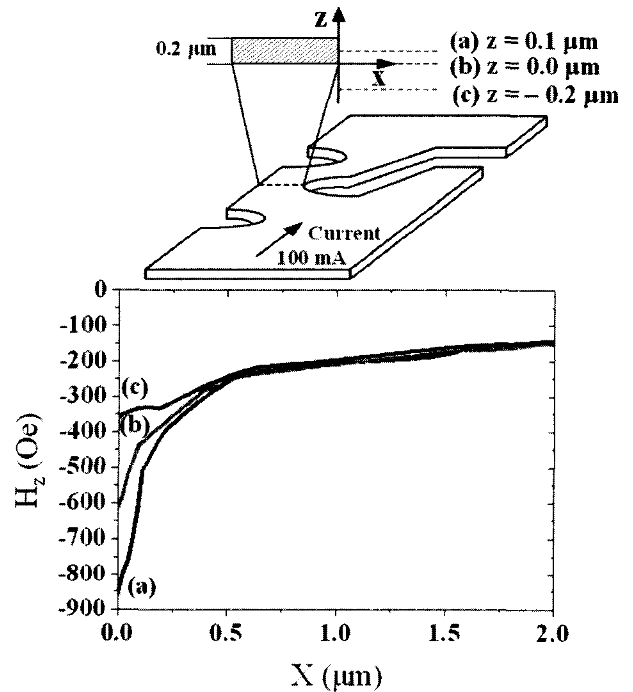

Fig. 4. Perpendicular magnetic field H_z produced by Y drive line of the new R-MOSLM carrying 100 mA current.

buried the MO film in order to take advantage of the maximum H_z produced at the center of the conductor with the aim of reducing the current of the drive line. However, for the new R-MOSLM, the perpendicular magnetic field H_z at the center of the conductor ((a) of Fig. 4) was two times higher than that for the conventional R-MOSLM

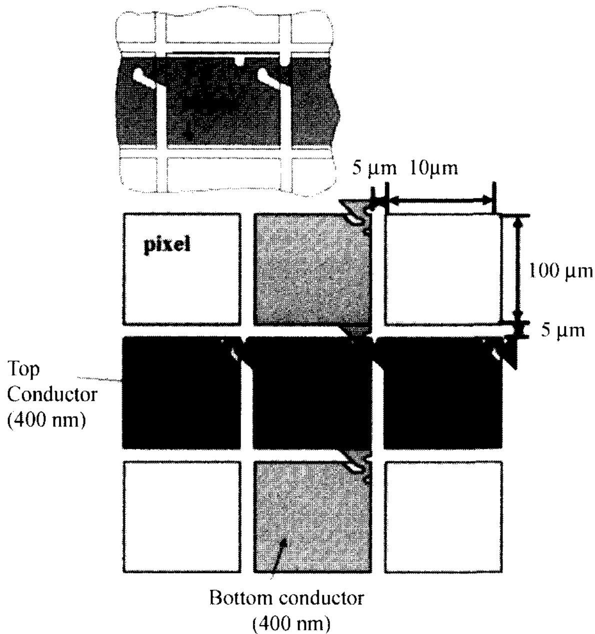

Fig. 5. Schematic of the new R-MOSLM with a wedge-shaped drive lines.

((a) of Fig. 3). The H_z at the bottom surface of the conductor for the new R-MOSLM ((b) of Fig. 4) was even considerably higher than that of the center of the conductor for the conventional R-MOSLM ((a) of Fig. 3). It is possible that the new R-MOSLM has a structure in which the conductor is not buried the MO film. The newly designed MOSLM enables simple processes due to the lack of rectangular channels in the MO film and the lack of buried conductors. Also, this results show that the switching sensitivity can be improved by decreasing the driving current and power loss using a conductor with a wedge.

The new reflective MOSLM is specially designed to have a wedge-shaped drive line and to cover the pixels as much as possible by X-Y drive lines, serving as a mirror layer. Figure 5 shows a schematic of new wedge-shaped R-MOSLM. The wedge-shaped conductors make it possible to have a lower power loss and a higher pixel fill factor (the ratio of the reflecting conductor area to the total area). The maximum perpendicular magnetic field is produced inside the corner of wedge of the conductor because the current density in the conductor has a larger value at the corner part of the wedge of the conductor. This indicates that the distribution of current density can be controlled by the shape of the conductor.

The new R-MOSLM has a layer structure of substrate/magnetic garnet/Al/SiO_2/Al. The substrate was a Czochralski grown single-crystal gadolinium gallium garnet with Ca, Mg and Zr substitution to expand the crystallographic

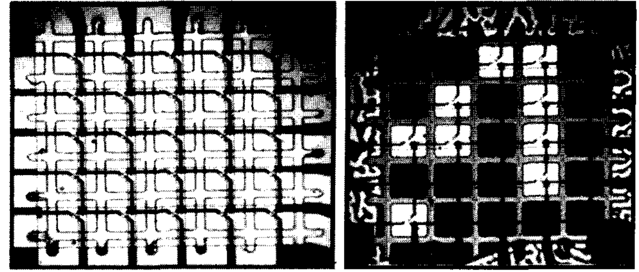

Fig. 6. Optical micrograph of the wedge-shaped R-MOSLM.

lattice. The bismuth-substituted iron garnet film was grown on the substrate by LPE. The garnet film possesses a perpendicular magnetization normal to the film plane induced by its uniaxial crystallographic structure. The thickness of the garnet film was about 5 μm. The film was structured into square pixels (mesas) by wet etching or ion milling. The number of pixels was $5 \times 5 = 25$. The pixels were 100×100 μm square wide and the pixel gap was 5 μm. Since the pixel gaps are as deep as 5 μm, 5 layers of polymer are spun on and baked until a flat surface is obtained. The polymer layer is then ion milled or polished. An Al layer 0.4 μm thick as the X conductor is ion-beam sputter-deposited on a patterned image reverse photoresist and a lift-off process is performed. The X conductor lies directly on the mesa surface and thus also plays the role of the optical mirror. A SiO_2 layer 0.4 μm thick as an insulator layer is deposited over the entire device opening only at the bonding pads of the X conductor to provide an insulator between X-Y conductors. An Al layer 0.4 μm thick as the Y conductor is patterned across the wedge of X-Y conductors. Figure 6 shows an optical micrograph of the wedge-shaped R-MOSLM. Finally, as a passivation layer, a polymer layer 5 μm thick is deposited over the entire device and removed from the bonding pads, and then the dicing and wire bonding are carried out.

For the dynamic switching test, a current pulse is sent through an X or Y drive line and the amplitude and width of the pulse to switch a pixel are measured. Figures 7(a) (c), and (e) show that when the current pulse is sent through the drive line with no bias field, the pixel is demagnetized. By maintaining a small external bias field of 40 Oe until the domain wall of the demagnetized pixel has propagated to all corners, the pixel switching is completed and the pixel is stable and remains in that state until the next nucleating process occurs. Figure 7 shows a single pixel, a row of pixels, and pixels shown in a capital "M" which was saturated with a bias field of 40 Oe in conjunction with the driven pulse.

Although the minimum linewidth of the new R-MOSLM

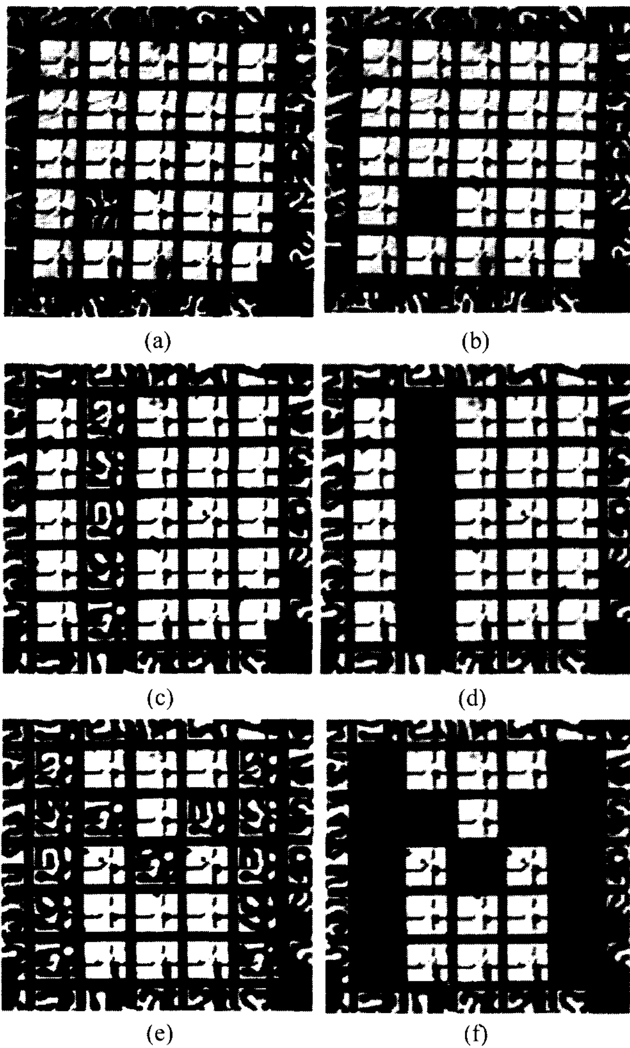

Fig. 7. shows a single pixel, a row of pixels, and pixels shown in a capital "M" which was saturated with a bias field of 40 Oe in conjunction with the driven pulse.

is three times larger than that of the conventional R-MOSLM, the X-Y driving current of the new R-MOSLM to demagnetize the pixel is almost equal to that of the conventional R-MOSLM at a current pulse width of 10 μs. These results indicate that if the minimum linewidth of the new R-MOSLM is equal to the minimum linewidth of the conventional R-MOSLM, the new R-MOSLM can be operated by a three times-smaller X-Y driving current because a current density three times larger is generated by the three times-reduced minimum linewidth. In other words, improvements by a factor of three in pixel switching sensitivity and power consumption, compared to the conventional R-MOSLM, can be achieved by the use of a wedge-shaped drive line.

3.2. Field-driven MOSLM

A novel MOSLM driven by an electric field is first fabricated by using the electrostrictive effect of PZT thin film. As the stress field induced by the PZT thin film reduces the anisotropy energy of the structured garnet film, we find that the pixels can be easily switched in accordance with or without the small external bias field. The field-driven MOSLM overcomes the thermal problems of the conductors that occur in the current-addressed driving method, and can provide high frame rates due to the high speed of the PZT thin film, and higher resolution due to simpler conductor structure.

The field-driven MOSLM had a layer structure of substrate/geometric magnetic garnet layer/(Ti)/Pt/elctrostrictive layer/Al. Figure 8 shows a schematic of a structure of the field-driven MOSLM and its cross section. The thickness of the garnet film is about 5 μm. The geometric pixel was formed by chemically etching the grooves into the garnet film layer. The geometric pixel dimensions are 100 μm $\times$ 100 μm, and the center-to-center separation between pixels is 105 μm. The total number of pixels is 5 $\times$ 5 = 25. Since the depth of the pixel groove is about 5 μm, the pixel groove must be planarized to allow the deposit of a lower conductor line. In the case of the conventional MOSLM, a polymer is used to planarize its groove. For the field-driven MOSLM, however, it is impossible to perform the planarization process by the conventional method, because an annealing process at 650 °C is required to crystallize the electrostrictive film. Therefore, a SiO_2 layer that survives in high temperature

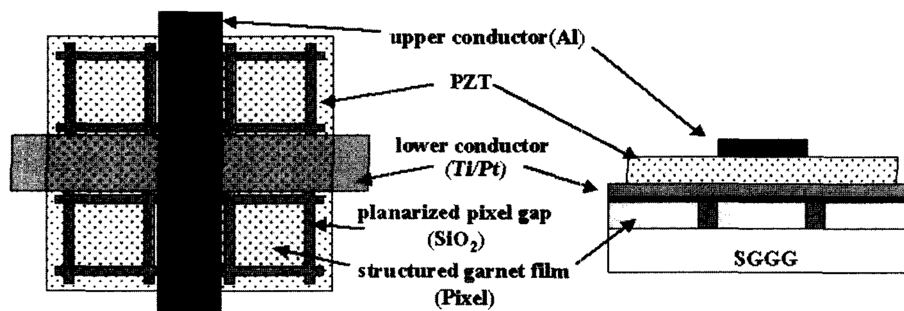

Fig. 8. Schematic of the MOSLM's structure and its cross section.

is used. The 6-μm thick SiO_2 layer is deposited by RF-magnetron sputtering and polished until a flat surface is obtained. A lower conductor line lies directly on the mechanically planed-surface of the garnet layer and thus also plays the role of the optical mirror. The 90-μm wide lower conductor line has a double layer that includes a Ti layer (thickness: 15 nm) and a Pt layer (thickness: 400 nm) which are ion-beam sputter-deposited on a patterned image reverse photoresist after which a lift-off process is performed. For the lower conductor line, the Ti layer is not necessary. A PZT ($Pb(Zr_{0.52}Ti_{0.48})O_3$) film acting as an electrostrictive layer, is prepared by a conventional sol-gel method on the patterned bottom conductors. The sol-gel solution was made by the Kanto Chemical Corporation. After spin coating the PZT precursor, the films were baked at 180 °C to evaporate the solvent and pre-annealed at 400 °C in dry air to eliminate organic components. These processes were repeated 3 times, then the films were crystallized by the rapid thermal annealing method at 650 °C. These processes were repeated twice. The deposited film thickness was about 780 nm. A 400-nm thick Al upper conductor line is then ion-beam sputtered and patterned. The lower and upper conductor lines, which were isolated by the PZT layer, were arranged as an X-Y matrix on a pixel. Figure 4 shows an optical micrograph of the fabricated MOSLM. Finally, as a passive layer, a 5-μm thick polymer layer was deposited on the parts of the device where the bonding pads had been removed. Finally, dicing and wire bonding were done.

The operation of the new field-driven MOSLM is based on a principle presented schematically in Fig. 9. First, entire pixels are magnetized in the "up" magnetization orientation by an external bias field in the "up" direction, which denotes that it is parallel to the light propagation, as shown in Fig. 9(a). When a voltage is applied through the conductor lines on a desired pixel, a stress generated by the electrostrictive layer only affects the selected geometric pixel. Klaus *et al.* had reported that the stress waves of an electrostrictive layer acting on small cells are equivalent to an effective magnetic field H_{eff} [12]. The H_{eff} is $3\lambda\sigma/M_s$ for a simple system, where λ is the magnetostrictive constant, σ is the stress and M_s is the saturation magnetization. This stress reduces the effect of the coercive field in the pixel, and in combination with heating, induces a change in the magnetic anisotrophy in the pixel, which is enough to enable the magnetized domains to realign to the plane of the garnet film (Fig. 9(b)). This in turn causes the stressed pixel to attain properties that make an easier switching of magnetization than the pixel without the stress. The pixel is easily switched in

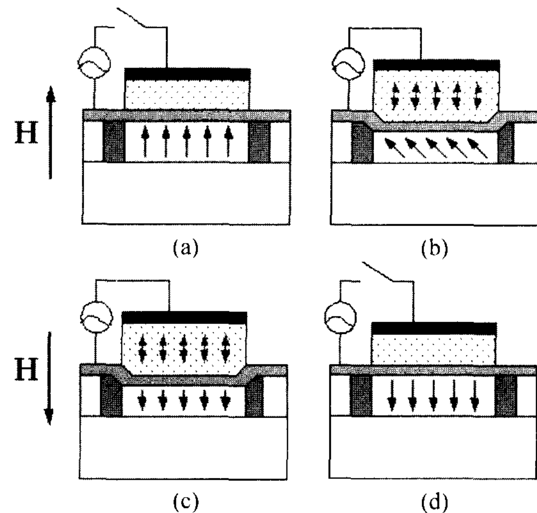

Fig. 9. Cross-sectional views for the device principle. (a) Initial phase saturated with the external bias field, (b) Intermediate phase applying voltage, (c) Phase applying the small bias field to complete a switching and (d) Phase to terminate selected pixel switching.

accordance with or without the small external bias field of the "down" direction as shown Fig. 9(c). Figure 9(d) shows the phase of the switched pixel with reverse magnetization, compared to Fig. 9(a).

Figure 10 shows the optical micrograph of the MOSLM saturated by an external bias field of 110 Oe. When peak-to-peak 8 V at the conductors A and B in Fig. 11(a) is applied with an external bias field of 40 Oe, the pixel is switched independently. Figure 11(b) shows an optical micrograph of the MOSLM switched to a checkerboard pattern.

3.3. Flat-surface MOSLM

We demonstrated a flat-surface MOSLM without physically isolated pixels and an external bias coil for the first time. The novel MOSLM, which was fabricated by a

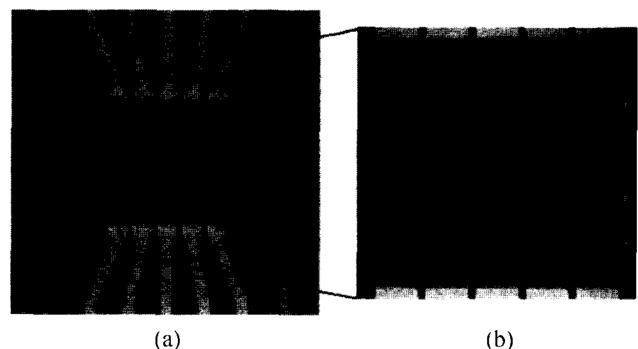

Fig. 10. (a) Optical micrographs of the MOSLM saturated by bias field of 110 Oe. (b) Magnified pixels of the MOSLM.

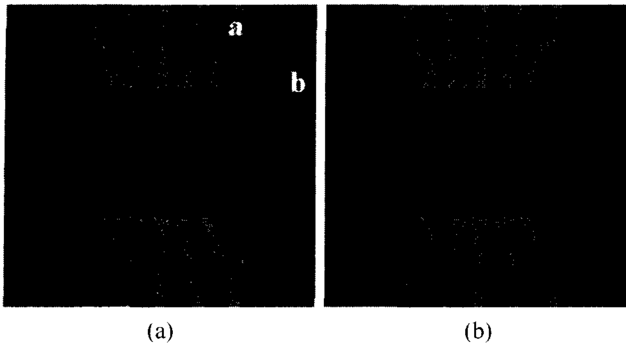

Fig. 11. Optical micrographs of (a) one switched-pixel and (b) nine switched-pixels of the MOSLM.

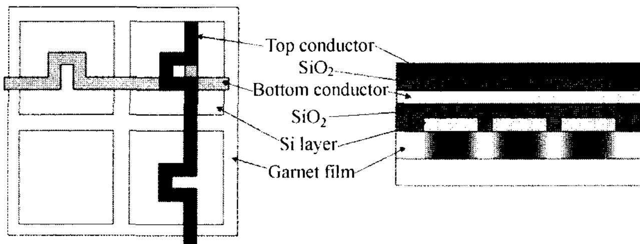

Fig. 12. Schematic of the structure of flat-surface MOSLM and its cross section.

simple process, was designed as a compact system with a high resolution and very low driving current. Flat-surface pixels for the novel MOSLM were produced by the combinatory use of the local annealing effect that reduced magnetization 4 πM_s of pixel areas and the stress effect that produced sharp variations of magnetic anisotropy in a magnetic garnet film under the edge of a metal layer.

Figure 12 shows a schematic of a structure of the novel flat-surface MOSLM and its cross section. As a substrate for the MOSLM, we used a Chocralski grown single crystal gadolinium gallium garnet (SGGG) boule with Ca, Mg and Zr substitution to expand a lattice constant. The novel MOSLM had the layer structure of substrate (SGGG) /magnetic garnet layer/space layer/patterned Si layer/ insulator layer/bottom conductor line/insulator layer/top conductor line, in turn.

A bi-substituted iron garnet film of $(BiGdY)_3$ $(FeGa)_5$ O_{12} was epitaxially grown on the substrate by liquid phase epitaxy methods; the garnet film possesses perpendicular magnetization normal to the film plane with a uniaxial crystallographic structure. The thickness of the grown magnetic garnet film was about 6 μm. The magnetic garnet layer was wet-etched in a H_3PO_4 and H_2SO_4 solution of 100 °C at an etching speed of 100 nm/min to obtain a suitable thickness of 3 μm. A thin SiO_2 layer with a thickness of 50 nm as a nonmagnetic space layer is deposited over the entire magnetic garnet layer. The thick space layer with a thickness of over 500 nm may reduce the stress field caused by the next overlying layer. A silicon layer with a thickness of 500 nm was ion beam sputter deposited and then patterned. The patterned silicon elements, which denote pixel areas, were 20 μm x 20 μm and the center-to-center separation between the elements was 25 μm. The total number of elements (pixels) was $16 \times 16 = 256$. The magnetic garnet film having the patterned silicon was annealed for 10 min at 900°C with thermal infrared (IR). The IR heats up only the garnet film areas beneath the patterned silicon elements. IR annealing is suitable for obtaining compact pixels with high resolution on the garnet film for the MOSLM, while the structure of a minute pixel with a fine gap was deformed by using laser annealing and electric furnace annealing. To more clearly isolate pixels, the samples were ion-milled for 10 min with milling rates of 200 nm for the garnet film and 300 nm for the Si layer, respectively. For a bottom conductor line, a SiO_2 layer with a thickness of 200 nm as the first insulator layer was deposited. An Al layer with a thickness of 400 nm as the bottom conductor line was ion beam sputtered and patterned. The width of the conductor lines which was laid at the center of the patterned silicon elements (pixels) was 2 μm. A SiO_2 layer with a thickness of 400 nm as the second insulator layer was deposited on the bottom conductor lines. An Al layer with a thickness of 400 nm as the top conductor line was fabricated by ion beam sputtering and patterning. The top and bottom conductor lines, which were isolated with the SiO_2 layer, were placed as a X-Y matrix on a pixel. Figure 13 shows the optical micrograph of bottom conductor lines deposited on the patterned silicon elements. Finally, as a passivation layer, a polymer layer with a thickness of 5 μm was

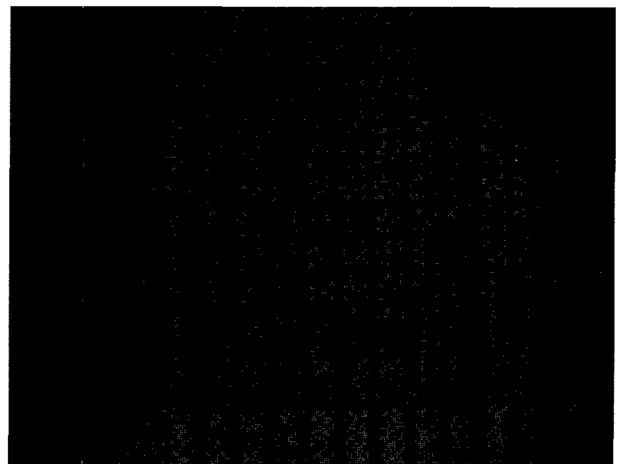

Fig. 13. Optical micrograph of bottom and top conductor lines deposited on the patterned silicon elements.

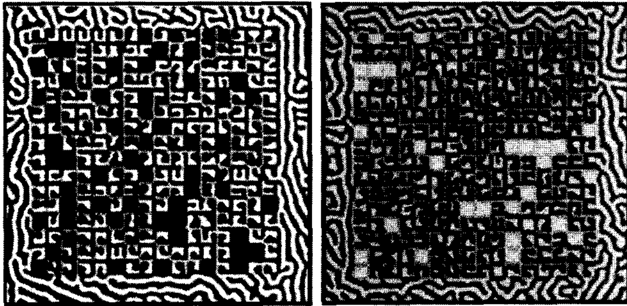

Fig. 14. Optical micrograph of magnetized pixels by stresses of patterned SI layers and external bias fields.

deposited over the entire device, where only the parts of the bonding pads were removed. Finally, dicing and wire bonding were carried out.

Flat-surface pixels for the novel MOSLM are produced by the combinatory use of the local annealing effect that reduced magnetization $4\pi M_s$ on the pixel areas and the stress effect that produced sharp variations of magnetic anisotropy in the magnetic garnet film under the edge of the metal layer. First, the rectangular edges of the patterned silicon elements generate the stress fields in the magnetic garnet layer, as described by Dishman *et al.* [13]. By such stress fields, the domain wall energy is substantially perturbed in the immediate vicinity of edges. This gives rise to either an attractive or a repulsive interaction, depending on the signs of the stress. The magnetic anisotropy is determined by the sum of the uniaxial anisotropy, the induced shape anisotropy, and the induced stress anisotropy. The induced stress anisotropy is varied by the stress induced by the patterned Si elements. Since the tension stress is positive and the compression stress is negative, the inner tension stress near the edge of the Si elements increases the magnetic anisotropy and the outer compression stress near the edge decreases the magnetic anisotropy. These sharp variations of magnetic anisotropy are effective for separating the pixels, as shown in Fig. 14.

Second, during the IR annealing process, the silicon layer, which is an oxidizable material, reduces oxygen from the surface of the LPE garnet film. The oxygen vacancies produce Fe^{2+} ions in the magnetic garnet film beneath the patterned silicon elements, due to transfer of gallium ions from tetrahedral (Ga^{3+}) to octahedral (Ga^{2+}) sites [14]. The presence of the resultant Fe^{2+} ions causes a decrease of magnetization $4\pi M_s$ in the magnetic garnet film, as shown in Fig. 15. That is, the areas in the garnet film beneath the patterned Si elements have roughly two times smaller magnetization $4\pi M_s$ than those without the patterned Si elements. Due to a difference of these magnetization $4\pi M_s$, the garnet film having a flat surface

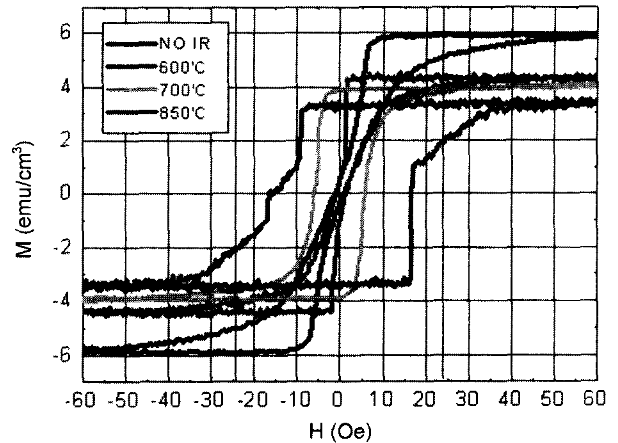

Fig. 15. Magnetic hysterisis loops of the garnet film with Si layer at IR annealing temperature of 0 °C, 600 °C, 700 °C, and 850 °C for 10 min.

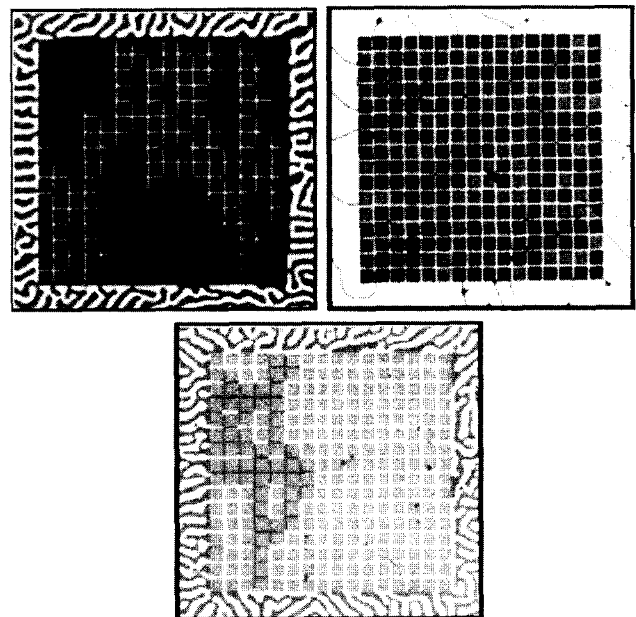

Fig. 16. Micrograph of the magnetized pixels at the novel MOSLM.

is magnetically isolated to become the pixels.

Figure 16 shows the micrograph of the pixels perfectly separated by two effects described above. Figure 17 shows the micrograph of switched pixels of the fabricated prototype MOSLM. The prototype MOSLM fabricated in this study is switched by applying currents of 6 mA for the bottom conductor line and 10 mA for the top conductor line. Such a driving current without an external bias field is over 10 times smaller than that of the conventional MOSLM which requires minimum currents of 70 mA and 150 mA for the bottom and top conductor lines, respectively. Since the novel flat-surface MOSLM can

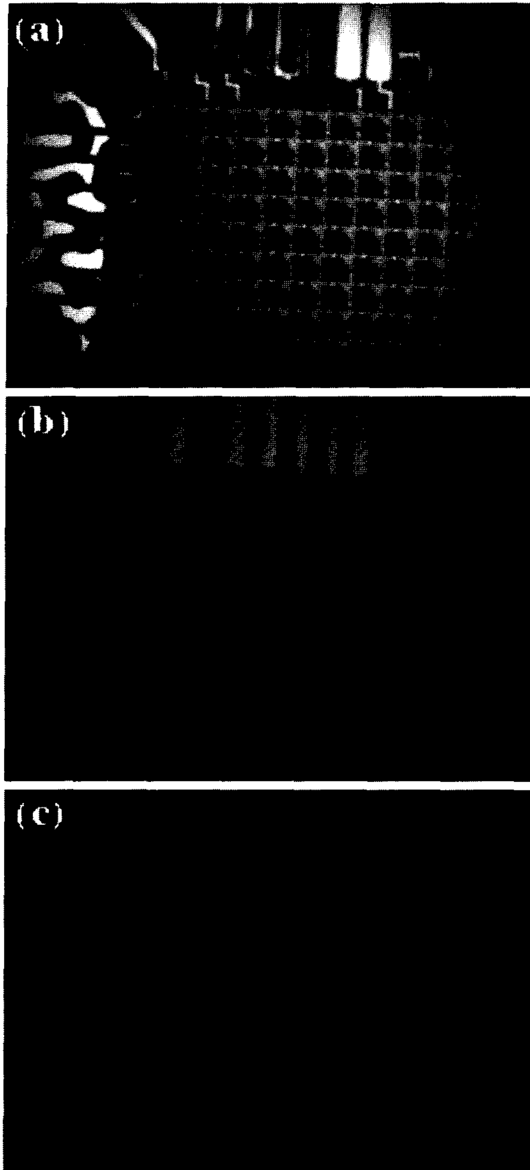

Fig. 17. Micrograph of switched pixels on the flat-surface MOSLM by applying currents of 6 mA for bottom conductor line and 10 mA for top conductor line, respectively. (a) Whole pixels, (b) a row of swithced pixels, and (c) a switched single pixel.

provide a high resolution, and a low driving current without an external bias coil, it is possible to be applied to the microdisplay such as ferroelectric liquid crystal SLM (FLC-SLM) and deformable mirror device (DMD).

4. Conclusions

We review recent development work on MOSLMs, mainly in relation to our own studies, including new type drive line for low driving current, voltage addressing method, and flat-surface pixel.

The new drive line for the R-MOSLM was designed using 3D electromagnetic field simulation and its prototype device was fabricated. The new R-MOSLM using the wedge-shaped conductor has a simple fabrication process and could achieve almost 100% window efficiency and one-third the driving current, compared to the conventional R-MOSLM. In particular, we mainly demonstrate new novel methods described as followed. One is a novel MOSLM driven by an electric field. The novel field-driven MOSLM can overcome the thermal problem of the conductor lines due to the voltage-addressed method by using the electrostrictive effect of PZT thin film, and provide high frame rate due to high speed of PZT thin film and high resolution due to simple conductor line structure. The other is a flat-surface MOSLM without the physically isolated pixels and external bias coil. Flat-surface pixels on the novel MOSLM were produced by the combinatory use of the infrared local annealing effect and the stress. The pixel of the MOSLM was switched by over ten times smaller driving current than that of the conventional MOSLM. The novel flat-surface MOSLM can provide higher resolution, simpler fabrication process, more compact systems and lower driving current than those of the conventional MOSLM. It is also possible to make the application for micro-displays like FLC-SLM and DMD.

Acknowledgments

The work was supported in part by the Grand-In-Aid from the Ministry of Education, Culture, Sport, and Technology of Japan.

References

[1] J. P. Kumme, H. Heitmann, D. Mateika, and K. Witter, J. Appl. Phys. **48**, 366 (1977).
[2] M. V. Longnov, V. V. Randshkin, Yu. N. Sazhin, V. P. Klin, B. P. Nam, and A. G. Soloviev, Sov. Phys. Tech. Phys. **36**, 493 (1991).
[3] W. E. Ross, D. Psaltis, and R. H. Anderson, Opt. Eng. **22**, 485 (1983).
[4] Nabil H. Farhat and Z. Y. Shae, Appl. Optics **28**, 4792 (1989).
[5] J. Cho, S. Santhanam, T. Le, K. Mountfield, D. N. Lambeth, D. Stancil, W. E. Ross, and J. Lucas, J. Appl. Phys. **76**, 1910 (1994).
[6] J. H. Park, J. K. Cho, K. Nishimura, and M. Inoue, Jpn. J. Appl. Phys. **41**, 1813 (2002).
[7] J. H. Park, J. K. Cho, K. Nishimura, and M. Inoue, Jpn. J. Appl. Phys. **41**, 2548 (2002).
[8] J. H. Park, D. H. Lee, J. K. Cho, K. Nishimura, and M. Inoue, J. Appl. Phys. **91**, 7014 (2002).

[9] Jae-Hyuk Park, H. Takagi, Dong-Hoon Lee and Jae-Kyeong Cho, K. Nishimura, H. Uchida and M. Inoue, J. Appl. Phys. 93 (2003), in press.
[10] Jae-Hyuk Park, H. Takagi, Jae-Hak Park and Jae-Kyeong Cho, K. Nishimura, H. Uchida and M. Inoue, J. Appl. Phys. 93 (2003), in press.
[11] Jaehyuk Park, H. Takagi, Jaehak Park, Jaekyeong Cho, K. Nishimura and M. Inoue, Jpn. J. Appl. Phys. **42**, (2003) No. 4B, in press.
[12] Klaus Schroder, J. Appl. Phys. **53**, 2759 (1982).
[13] J. M. Dishman, R. D. Pierce, and B. J. Roman: J. Appl. Phys. **45**, 4076 (1974).
[14] P. H. L. Rasky, D. W. Gerve, and M. H. Kryder, J. Appl. Phys. **57**, 4077 (1985).